UV−Vis Spectrophotometric Titrations and Vibrational Spectroscopic Characterization of *meso*-(*p*-Hydroxyphenyl)porphyrins

Hongwei Guo,[†] Junguang Jiang,[†] Yingyan Shi,[‡] Yuling Wang,[†] Jiannan Liu,[†] and Shaojun Dong*,[†]

State Key Laboratory of Electroanalytical Chemistry, Changchun Institute of Applied Chemistry, Chinese Academy of Sciences, Changchun, Jilin, 130022, P. R. China, and Department of Chemistry, Jilin University, Changchun, Jilin, 130023, P. R. China

Received: March 6, 2004; In Final Form: April 21, 2004

Sequentially spectrophotometric titrations by sodium hydroxide of meso-tetraphenylporphyrin derivatives bearing one, two, three, or four p-hydroxyl groups result in new types of spectra. The strong new bands appear in the visible region with splitting or broadening of the Soret band and its significant loss of oscillator strength. To understand the molecular origin of these phenomena, the Resonance Raman (RR) and Fourier Transform Infrared (FTIR) experiments are carried out. The results demonstrate that the charges of the deprotonated para-hydroxy substituted meso-tetraphenylporphyrins are localized on the substituents, not delocalized into the π system of the porphyrin macrocycles and that the ground states of the macrocycles remain essentially unperturbed. Both the related behavior of diprotonated tetrakis(p-(dimethylamino)phenyl) porphyrin and protonated Schiff base porphyrins show that the new bands considered as *hyperporphyrin* spectra are due to π(phenoxide anion) $\rightarrow \pi^*$(porphyrin) transitions, where π is an orbital on the phenoxide anion substitutent and π^* is a LUMO on the porphyrin.

1. Introduction

The importance of porphyrins in nature[1] and in technical applications has led to electronic absorption and other spectroscopic studies of these compounds. In the ultraviolet−visible region, the characteristic spectra of porphyrins including the intense Soret band around 400 nm and a series of bands (Q-bands) through the visible region are usually well-described by the so-called four-orbital model.[2,3] This ascribes the ground-state absorptions of porphyrins as transitions to $^1(\pi, \pi^*)$ states derived from $[a_{1u}(\pi), e_g(\pi^*)]$ and $[a_{2u}(\pi), e_g(\pi^*)]$ configurations, where $a_{1u}(\pi)$ and $a_{2u}(\pi)$ are the nearly degenerate porphyrin ring highest occupied molecular orbital (HOMOs) and $e_g(\pi^*)$ are the degenerate ring lowest unoccupied molecular orbital (LUMOs), respectively. Mixing of these configurations gives rise to the strongly allowed, near-UV Soret band and the quasi-allowed, less-intense, lower-energy Q-bands. The effects of peripheral or central substitutions on the optical properties of porphyrins can generally be explained by slight energy shifts of these transitions.

However, some substitutions of the central metal or on the ring of porphyrins have led to unusually-spectroscopic effects that require additional interpretation. Some metalloporphyrins have been know to show some extra absorption bands in the region $\lambda > 320$ nm.[3] Certain para-hydroxy TPP derivatives such as meso-tetrakis(3,5-di-*tert*-butyl-4-hydroxyphenyl)porphrin[4] in basic solution have shown numerous spectral and structural features, complicated by accompanying redox processes leading to quinonelike structures. The partial protonation of para-amino-substituted meso-tetraphenylporphyrins leads to broadened, or even "split", Soret bands and strongly enhanced and red-shifted absorption in the visible region.[5−8] For example, the diprotonated form of tetrakis(p-(dimethylamino)phenyl)porphyrin shows a sharply split Soret band and a unusually intense red band. Such molecules have been described as *hyperporphyrins*.

Hyperporphyrins have been defined as porphyrins that exhibit prominent extra absorption bands ($\epsilon > 1000$ M^{-1} cm^{-1}) in the region $\lambda > 320$ nm which are not porphyrin $\pi-\pi^*$ transitions.[3] These extra bands are often due to charge transfer (CT) interactions of porphyrins with either metal orbitals or substituents. In diprotonated meso-tetrakis(p-(dimethylamino)phenyl)-porphyrin, molecular orbital calculations[9] suggest that the *hyperporphyrin* transitions are of π(phenylamine) $\rightarrow \pi^*$(porphyrin) origin, where π(phenylamine) is an orbital on the phenylamine substitutent and π^*(porphyrin) is a LUMO on the porphyrin. To better extend these observations, in the present study, sequentially spectrophotometric titrations of mono-, di-, tri-, and tetra-p-hydroxy substituted meso-tetraphenylporphyrins by sodium hydroxide are carried out. RR and FTIR data presented here provide essential evidence necessary for further understanding of the molecular origins of the spectral changes upon deprotonation.

2. Experimental Section

Materials. The porphyrins were prepared and characterized by previously described methods[10] as follows. For abbreviations, we use the notation $(OH)_m(ONa)_nPH_2$, where *m* is the number of para-hydroxy-substituted phenyls and *n* is the number of deprotonated para-hydroxy-substituted phenyls. The notation and substitution patterns of these porphyrins are shown in Figure 1.

Analytical grade N, N-dimethylformamide (DMF) was dried over activated molecular sieves (4 Å) for 24 h and then was distilled under reduced pressure prior to use. Doubly-distilled

* Corresponding author. Fax: +86-431-5689-711. E-mail: dongsj@ns.ciac.jl.cn.
[†] Chinese Academy of Sciences.
[‡] Department of Chemistry, Jilin University.

10.1021/jp048981f CCC: $27.50
Published on Web 06/08/2004

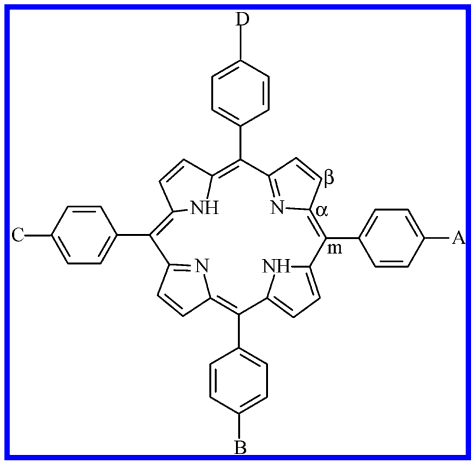

Figure 1. Structure of substituted free-base porphyrins. Porphyrin substitution patterns (**I**) $(OH)_1PH_2$ A=OH B=C=D=H; (**II**) $(OH)_2PH_2$ A=B=OH C=D=H; (**III**) $(OH)_3PH_2$ A=B=C=OH D=H; (**IV**) $(OH)_4PH_2$ A=B=C=D=OH.

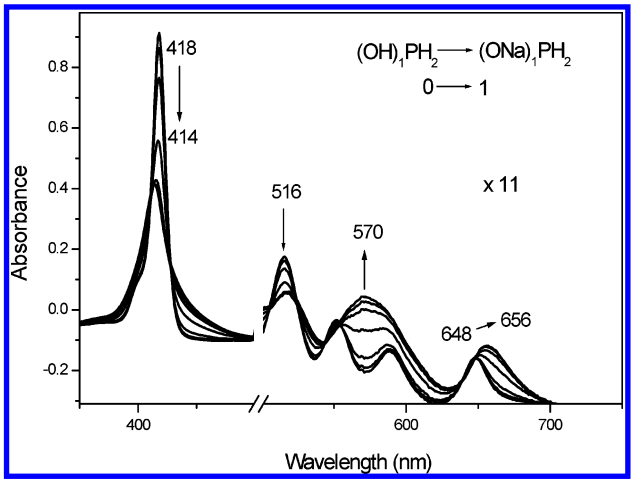

Figure 2. Spectrophotometric titration of $(OH)_1PH_2$ with NaOH. 0 → 1 indicates the neutralization of one proton. The × 11 is the scale factor used for Q-bands.

water was used in all sample preparations. All other chemicals used were analytical grade and were used as received.

A Series of Meso-(p-hydroxyphenyl)porphyrins. Samples of p-hydroxylbenzaldehyde (5.3 g, 43.4 mmol, 0.174 M) and benzaldehyde (11.5 mL, 0.115 mol, 0.46 M) were dissolved in 250 mL of propionic acid, and then the solution was vigorously stirred and heated to reflux. Pyrrole (10.6 mL, 0.153 mol, 0.612 M) was then added dropwise. After completion of addition, the mixture was refluxed a further 1.5 h. The reaction mixture was then stirred and cooled to room temperature. The cooled solution was left overnight, and then the mixture was neutralized with NaOH and filtered at reduced pressure to give a dark purple powder. This powder was placed on top of a silica gel column (Si 60−100 mesh) poured with chloroform. The porphyrins were eluted using chloroform followed by ethanol/chloroform in different ratios. Further separation via thin-layer chromatography afforded meso-tetraphenylporphyrin (**$TPPH_2$=$(OH)_0PH_2$**), 5,10,15-triphenyl-20-(4-hydroxyphenyl)porphyrin (**I=$(OH)_1PH_2$**), 5,15-diphenyl-10,20-bis(4-hydroxyphenyl)porphyrin (**trans-$(OH)_2PH_2$**), 5,10-diphenyl-15,20-bis(4-hydroxyphenyl) porphyrin (**II=cis-$(OH)_2PH_2$**), 5-Phenyl-10,15,20-tri(4-hydroxyphenyl)-porphyrin (**III=$(OH)_3PH_2$**), and meso-tetrakis(4-hydroxyphenyl)-porphyrin (**IV=$(OH)_4PH_2$**): ^{1}H NMR (DMSO−d_6) (**I**) δ -2.79 (s, 2H, NH), 7.32 ∼ 7.34 (d, 2H, m−C_6H_4OH), 7.91 ∼ 7.96 (m, 9H, m, p−C_6H_5), 8.12 ∼ 8.14 (d, 2H, o−C_6H_4OH), 8.32 ∼ 8.34 (t, 6H, o−C_6H_5), 8.93 ∼ 9.04 (m, 8H, CH_2), 10.13 (s, 1H, OH); (**II**) δ -2.80 (s, 2H, NH), 7.32 ∼ 7.34 (d, 4H, m−C_6H_4OH), 7.94 ∼ 7.96 (d, 6H, m, p−C_6H_5), 8.12 ∼ 8.14 (d, 4H, o−C_6H_4OH), 8.33 ∼ 8.34 (t, 4H, o−C_6H_5), 8.93 (s, 4H, CH_2), 9.02 (s, 4H, CH_2), 10.12 (s, 2H, OH); (**III**) δ -2.79 (s, 2H, NH), 7.32 ∼ 7.35 (m, 6H, m−C_6H_4OH), 7.93 ∼ 7.95 (d, 3H, m, p−C_6H_5), 8.12 ∼ 8.15 (m, 6H, o−C_6H_4OH), 8.32 ∼ 8.34 (t, 2H, o−C_6H_5), 8.92 (d, 2H, CH_2), 9.01 (s, 6H, CH_2), 10.11 ∼ 10.12 (d, 3H, OH); (**IV**) δ -2.78 (s, 2H, NH), 7.32 ∼ 7.34 (d, 8H, m−C_6H_4OH), 8.11 ∼ 8.13 (d, 8H, o−C_6H_4OH), 8.99 (s, 8H, CH_2), 10.10 (s, 4H, OH); absorbance (CH_2Cl_2): (**I**) 418.40, 515.68, 547.68, 589.92, 647.52 nm; (**II**) 419.68, 515.68, 550.24, 592.48, 648.80 nm; (**III**) 418.40, 515.68, 552.80, 592.48, 648.80 nm; (**IV**) 419.68, 518.24, 554.08, 593.76, 648.80 nm;

Spectroscopy. UV−Visible absorption spectra were taken on a Cary 500 Scan UV−Vis−NIR spectrophotometer (Varian, United States) using a 2 mm slit width. Data acquisition was via a GPIB card and a PC using Cary Win UV software. RR spectra were recorded with a J−Y T64000 laser Raman instrument. Laser excitation at 514.5 nm was obtained with a Spectra Physics 2017 argon ion laser. All spectra were collected at backscattering geometry at room temperature. Incident powers were 20−50 mW. Optical spectra were recorded before and after each RR experiment on a Cary 500 spectrophotometer to ensure that the samples had not decomposed. Baseline corrections were carried out using Labspec (J−Y) software (ver 3.03T). FT−IR spectra were obtained with a Bruker IFS-66v/S (Germany) FT−IR spectrometer. The spectral resolution was set at 2 cm^{-1}. The average scan times were 100. For all samples, the AquaSpec Flow Cell (Micro-biolytics Company, Germany) with calcium fluoride windows was used, and the light length was 6 μm.

UV−Vis Spectrophotometric Titration. Solutions of porphyrins in DMF + H_2O (V: V = 1:1) mixture were titrated directly in 1-cm absorption cells by successive additions of sodium hydroxide while monitoring the spectra between 350 and 750 nm. Increasingly concentrated NaOH (0.1−10 M) solution was added in 2 to 10 μL aliquots using a microliter syringe. The original porphyrin solution was ∼ 4 μM in a total volume of 3.0 mL. The total volume change during the titration was negligible. After addition of each aliquot, the cell was capped and mixed by inversion and the spectrum was retaken. In all cases, the reversibility of the deprotonation was demonstrated by the addition of 4.0 M HCl.

3. Results

3.1 UV−Vis Spectrophotometric Titration. Figures 2−5 present spectrophotometric titrations for $(OH)_1PH_2$, $(OH)_2PH_2$, $(OH)_3PH_2$, and $(OH)_4PH_2$. Deprotonation of the para-hydroxyphenyl substituents of these compounds has been shown to induce dramatic change in the optical spectra. Comparing the spectral changes of these four species during the titration, we can find that species with the same number of peripheral phenoxide anion substituents have similar spectra. Hence, these titration procedures can be roughly resolved into four steps due to somewhat overlapping deprotonation. The initial products, assigned to these species with one phenoxide anion substituent (0 → 1; solid lines in Figure 2, 3, 4A, and 5A), show a markedly reduced, broadened, and slightly blue-shifted Soret peak, the reduced height of the O_y(1,0) band and two new bands, a very broad canopy-like strong band at around 570 nm, and a strong red band at around 656 nm. The second step (1 → 2; dashed lines in Figure 3, 4A, and 5A) at higher concentrated NaOH deprotonates the second peripheral hydroxyl, giving a "split

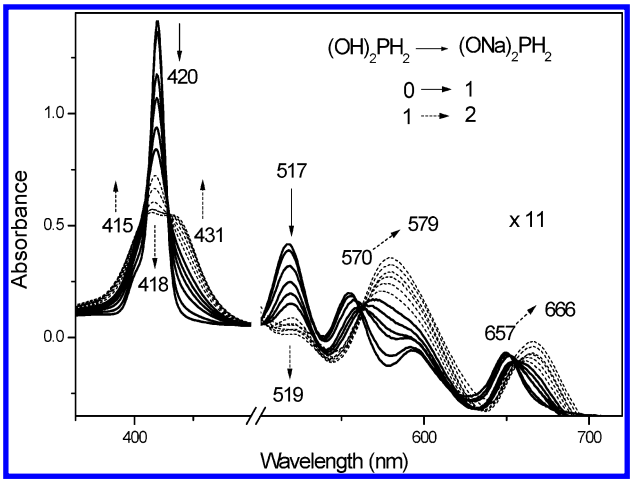

Figure 3. Spectrophotometric titration of $(OH)_2PH_2$ with NaOH. 0 → 1(solid lines) and 1 → 2 (dashed lines) indicate the neutralization of the first proton and the second proton. The × 11 is the scale factor used for Q-bands.

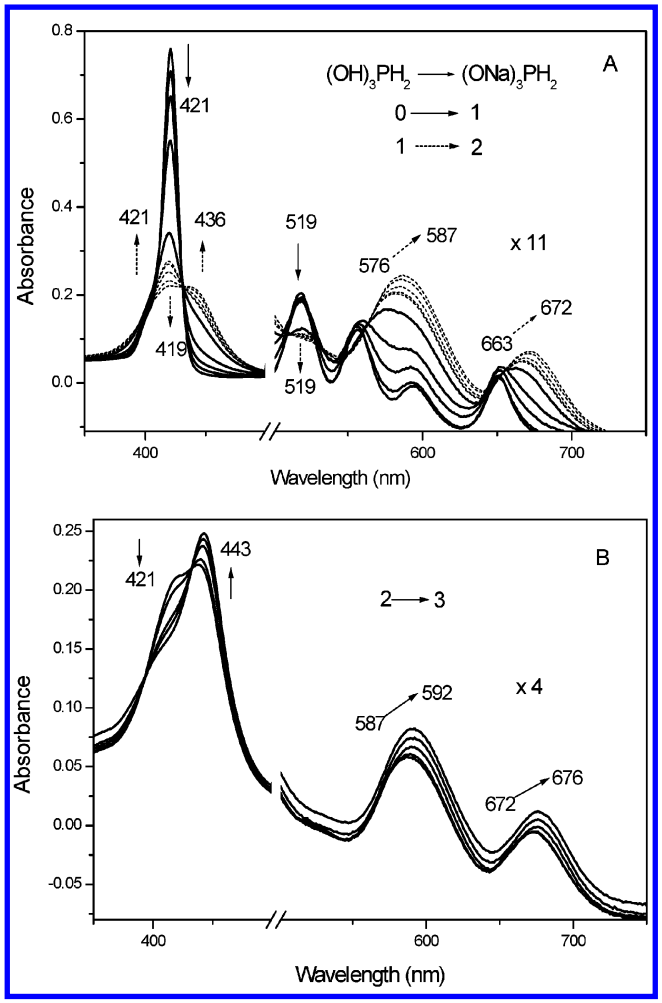

Figure 4. Spectrophotometric titration of $(OH)_3PH_2$ with NaOH. (A) 0 → 1 (solid lines) and 1 → 2 (dashed lines) indicate the neutralization of the first proton and the second proton. (B) 2 → 3 (solid lines) indicates the neutralization of the third proton. The × 11 and × 4 are the scale factors used for Q-bands.

Soret" structure in which two components have about equal height. The reduced $O_y(1,0)$ band disappears, and two new bands at 579 nm and at 666 nm in Figure 3 move to 587 and 672 nm in Figure 4A, move further to the red in Figure 5A (to 588 and 674 nm), and increase in height. During this stage, the spectral

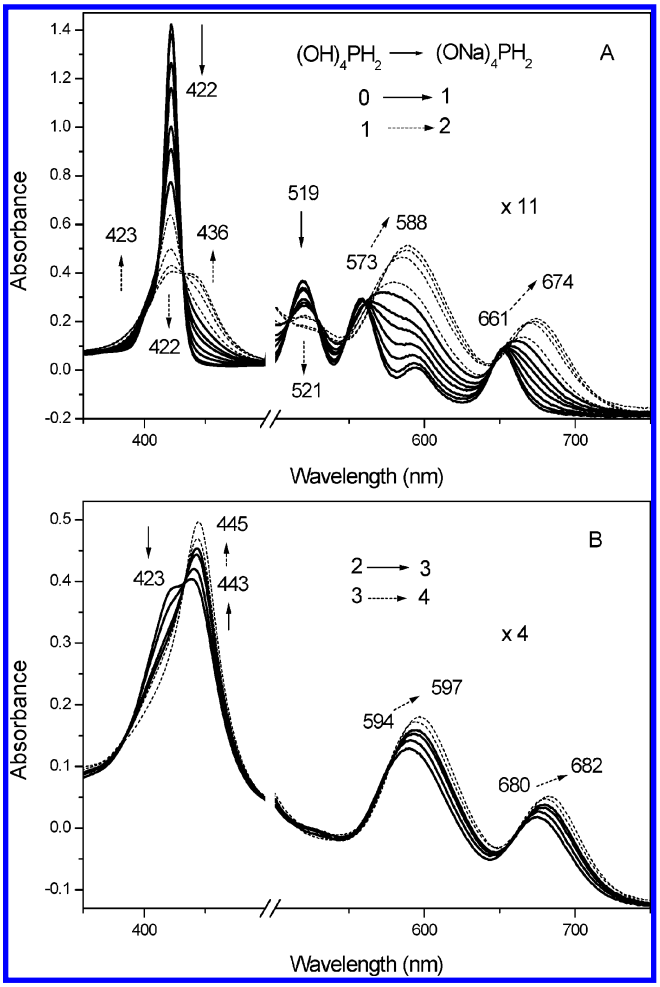

Figure 5. Spectrophotometric titration of $(OH)_4PH_2$ with NaOH. (A) 0 → 1 (solid lines) and 1 → 2 (dashed lines) indicate the neutralization of the first proton and the second proton. (B) 2 → 3 (solid lines) and 3 → 4 (dashed lines) indicate the neutralization of the third proton and the fourth proton. The × 11 and × 4 are the scale factors used for Q-bands.

change of $(OH)_2PH_2$ slightly differs from that of $(OH)_3PH_2$ and $(OH)_4PH_2$. The main reason may be that $(OH)_3PH_2$ and $(OH)_4$-PH_2 are apt to form the two " trans" (i.e., on opposite sides of the macrocyclic skeleton), not "cis" (i.e., on adjacent sides of the macrocyclic skeleton), phenoxide anion substituents in $(OH)_2PH_2$ (Scheme 1).[4,11] In the third step, (2 → 3; solid lines in Figure 4B and 5B), the short-wave component of the "split Soret" disappears, the low-energy component moves to 443 nm and increases slightly in height, and the two new bands move to the red (592 nm, 676 nm in Figure 4B and 594 nm, 680 nm in Figure 5B) and continue to increase in height. The final deprotonation
(3 → 4; dashed lines in Figure 5B) forms a three-band spectrum similar to that in the acidic solution, with a Soret peak (at 445 nm) and two red-shifted, markedly-enhanced new bands at 597 and 682 nm.

3.2 The Resonance Raman and FTIR Spectra. Figure 6 shows the high-frequency region (1000−1700 cm^{-1}) RR spectra obtained for $(OH)_1PH_2$, $(OH)_2PH_2$, $(OH)_3PH_2$, and $(OH)_4PH_2$ in neutral and basic DMF + H_2O (V:V = 1:1) mixture using a 514.5 nm excitation. In this region, it is well-known that the RR spectra of TPP derivatives are usually dominated with porphyrin skeletal modes due to a resonant effect, though the phenyl modes may be observed occasionally.[12] Using the normal coordinate analysis of meso-tetraphenylporphyrinato Ni (II), We

SCHEME 1

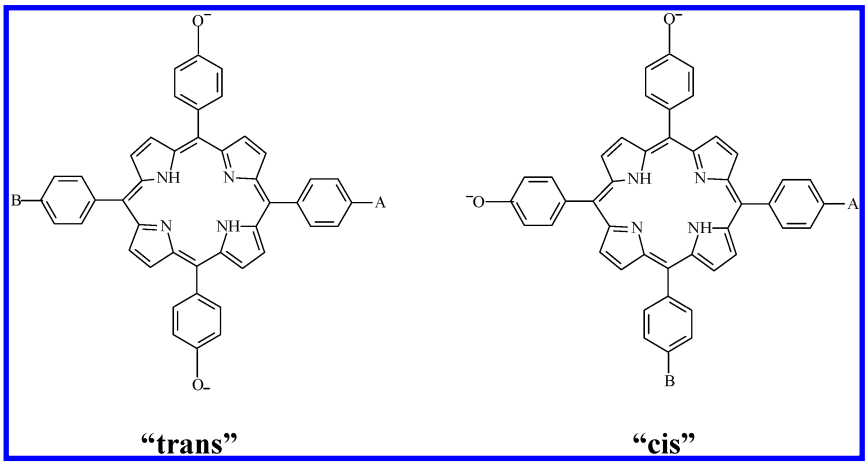

have collected several of the prominent vibrations of these species in Table 1 and assigned these in analogy with the results of Li et al.[13] The atom labeling is defined in the structural diagram (Figure 1).

In resonance with the Q-band (514.5 nm excitation) the RR spectrum is dominated by depolarized (dp) and anomalously polarized (ap) bands. They arise from B_{1g} or B_{2g} (dp) and A_{2g} (ap) modes which are vibronically active in Q−B mixing and are enhanced via the B (vibronic) term. In Figure 6 the RR spectra of $(OH)_1PH_2$, $(OH)_2PH_2$, $(OH)_3PH_2$, and $(OH)_4PH_2$ in neutral DMF + H_2O (1:1) show strong enhancement of non-totally symmetric modes at 1232−1238 cm^{-1} (ν_{26}) and 1543−1548 cm^{-1} (ν_{19}). Upon deprotonation the porphyrin skeletal vibrations are nearly unaffected; the band positions and the relative intensity of $(OH)_1PH_2$, $(OH)_2PH_2$, $(OH)_3PH_2$, and $(OH)_4PH_2$ are nearly identical under neutral versus basic conditions (about a 5 cm^{-1} change in ν_{11}, upon formation of peripheral phenoxide anion substituents, most likely arises from a slight porphyrin core expansion accompanying the deprotonation reaction[14]). We do not observe clearly identifiable phenyl modes that are internal to phenyl rings in all cases. To determine the changes of phenyl rings upon deprotonation, we carry out analogous FTIR experiments of $(OH)_4PH_2$ (only FTIR experiments of $(OH)_4PH_2$ are carried out due to the lower solubility of $(OH)_1PH_2$, $(OH)_2PH_2$, and $(OH)_3PH_2$ in neutral solution) in neutral and basic DMF + H_2O (V:V = 1:1) mixture (shown in Figure 7). Due to the low solubility of $(OH)_4PH_2$ in a neutral solution leading to a low signal-to-noise ratio, we only assign the main IR bands.[15] Upon deprotonation the frequency of the band at 1349 cm^{-1} assigned to the C_m-phenyl stretching vibration does not nearly change. The major changes are the phenyl C═C stretching frequency at 1611 cm^{-1} that shifts down by 19 cm^{-1}, and the disappearance of the p-hydroxyphenyl C−O stretching frequency at 1234 cm^{-1}.[10] Presumably, the formation of phenoxide anion substituents should lead to the C−O stretching frequency shifted up due to delocalization of the negative charge onto the phenyl ring, which makes the bond length of the phenoxide anion normalized. To determine its exact peak position under basic conditions, FTIR spectra of a simple model system (phenol/phenolate) in DMF + H_2O (1:1) mixture are shown in Figure 8. Comparing Figure 7 with 8, very similar phenomena are observed. Upon deprotonation the C═C stretching vibration at ∼ 1600 cm^{-1} shifts down to 1589 cm^{-1} and the two peaks at 1238 and 1271 cm^{-1} disappear and combine into one peak (Figure 8). Hence, related to the band assignment of phenol/phenolate, the two peaks at 1234 and 1273 cm^{-1} are ascribed to C−O stretching and O−H bending,[16] respectively. Upon deprotonation, the O−H bending at 1273 cm^{-1} disappears and the C−O stretching at 1234 cm^{-1} shifts up to 1271 cm^{-1} (Figure 7).[17] The phenomena closely related to those described here occur in the case of metal complexes of Schiff base porphyrins (SB),[18] as follows (Scheme 2). RR measurements showed that protonation had very little effect on ring vibration frequencies but that protonation of the Schiff's base shifted up the N═C stretching frequency by 11 cm^{-1}. All the phenomena provide enough evidence that the negative center is not thoroughly delocalized throughout the π system, but rather deprotonation has the effect of generating an exceptionally strong electron-donating group.

4. Discussions

The P−OHTPPH_2 has ionizable protons (Hs) at the two centers, the comparatively acidic phenolic-Hs on the meso-hydroxyphenyl substituents in the peripheral region and the inner core pyrrolic-Hs on the two ═NH groups. The imino (═NH) groups are very weakly acidic[3] (pK > 15). Therefore, on titration with strong alkali only the P-hydroxyphenyl group is expected to ionize in the high pH range.[19] This has been inferred from the experiment[20] of deprotonation of free-base meso-tetrakis-(p-hydroxyphenyl)porphyrin ($(OH)_4PH_2$) and nickel (II) meso-tetrakis-(p-hydroxyphenyl)porphyrin ($Ni(OH)_4PH_2$). The same effect observed for both ($(OH)_4PH_2$) and ($Ni(OH)_4PH_2$) indicates that the spectral changes resulted from the deprotonation of the phenolic protons and not the ═NH protons of the free-base porphyrin.

As shown in Figures 2−5, for all four macrocycles the deprotonation results in the markedly red-shifted, strong new bands in the visible region, and increasing the number of peripheral phenoxide anion substituents increases the extent of the red shift of all bands. These dramatically spectral changes have been observed by Manna et al.[19] in a DMF + H_2O (1:1) mixture, for which they suggested the possibility of delocalization of these peripheral charges in solution along the conjugative pathways into the core region, causing an accumulation of negative charges only on the pyridine-type Ns. This new charge distribution due to the resonance effect will create a dipole with the positive pole on the phenolic oxygen in the meso-positions and the negative pole on the N in the center. Thus, a charge transfer state is created. But our RR and FTIR data demonstrate that the charges of the deprotonated para-hydroxy substituted meso-tetraphenylporphyrins are localized on the substituents, not delocalized into the π system of the porphyrin macrocycles and that the ground states of the

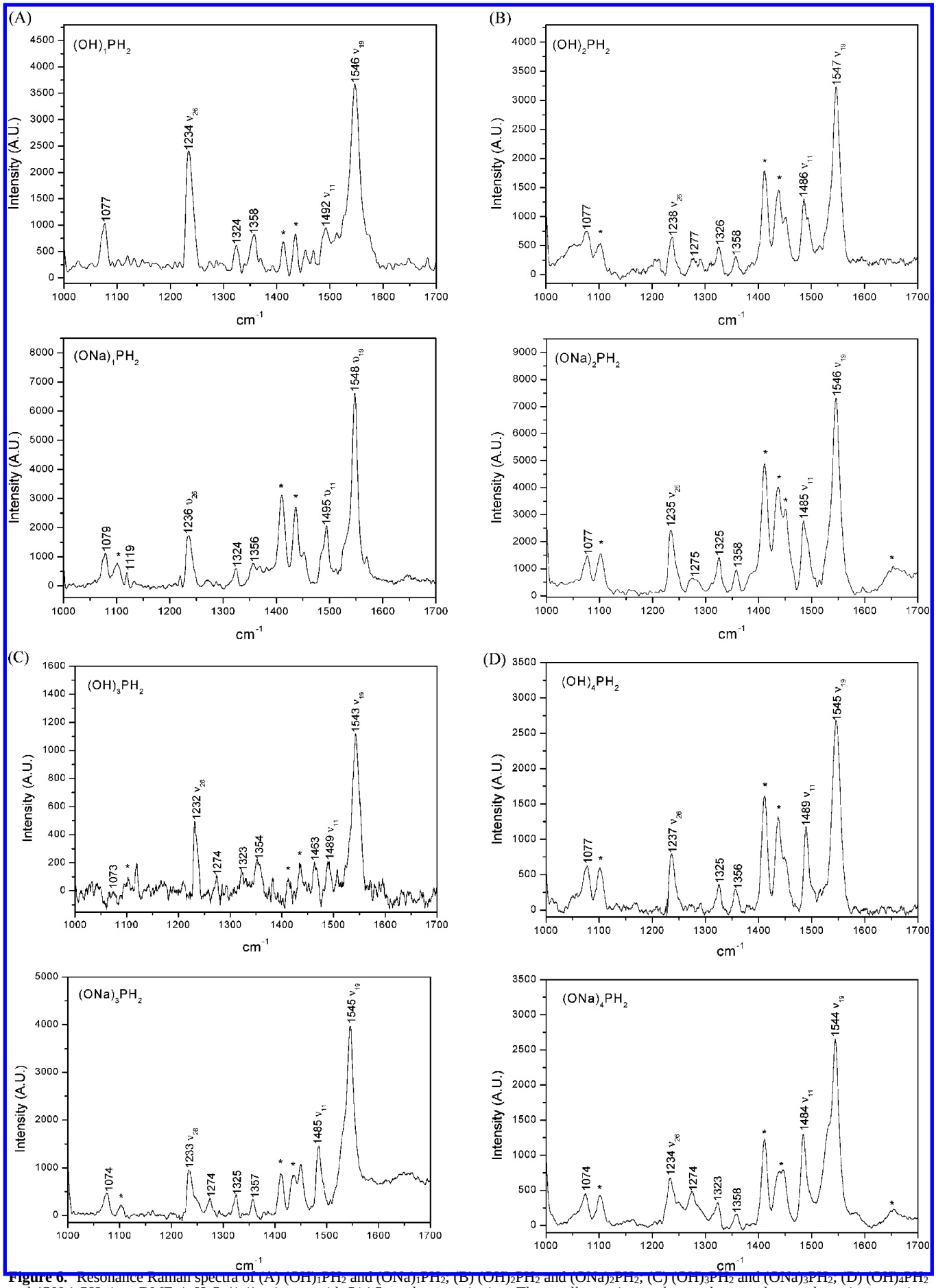

Figure 6. Resonance Raman spectra of (A) $(OH)_1PH_2$ and $(ONa)_1PH_2$, (B) $(OH)_2PH_2$ and $(ONa)_2PH_2$, (C) $(OH)_3PH_2$ and $(ONa)_3PH_2$, (D) $(OH)_4PH_2$ and $(ONa)_4PH_2$ in a DMF + H_2O (1:1) mixture with 514.5 nm laser excitation. The small negative peaks are due to solvent subtraction or noise. * =solvent band.

TABLE 1: Raman Frequency (cm^{-1}) of $(OH)_1PH_2$, $(OH)_2PH_2$, $(OH)_3PH_2$, and $(OH)_4PH_2$ in Neutral and Basic DMF + H_2O (V:V = 1:1) Mixture[a]

$(OH)_1PH_2$	$(ONa)_1PH_2$	$(OH)_2PH_2$	$(ONa)_2PH_2$	$(OH)_3PH_2$	$(ONa)_3PH_2$	$(OH)_4PH_2$	$(ONa)_4PH_2$	assignment[b]
1546	1548	1547	1546	1543	1545	1545	1544	$\nu(C_\alpha C_m) + \delta(C_\alpha C_m C_{Ph})$
1492	1495	1486	1485	1489	1485	1489	1484	$\nu(C_\beta C_\beta) + \delta(C_\beta H)$
1358	1356	1358	1358	1354	1357	1356	1358	$\nu(C_\alpha C_\beta) + \delta(C_\beta H) + \delta(C_\alpha C_\beta)$
1324	1324	1326	1325	1323	1325	1325	1323	$\nu(C_\alpha C_\beta) + \delta(C_\beta H)$
1234	1236	1238	1235	1232	1233	1237	1234	$\nu(NC_\alpha) + \nu(C_\alpha C_\beta) + \delta(C_\alpha C_\beta C_\beta) + \delta(C_\alpha C_m)$
1077	1079	1077	1077	1073	1074	1077	1074	$\delta(C_\beta H) + \nu(C_\beta C_\beta)$

[a] The concentration of $(OH)_1PH_2$, $(OH)_2PH_2$, $(OH)_3PH_2$ and $(OH)_4PH_2$ in neutral and basic DMF+H_2O (1:1) mixture is 5×10^{-4} M. [b] Assignments are based on those for NiTPP.[13]

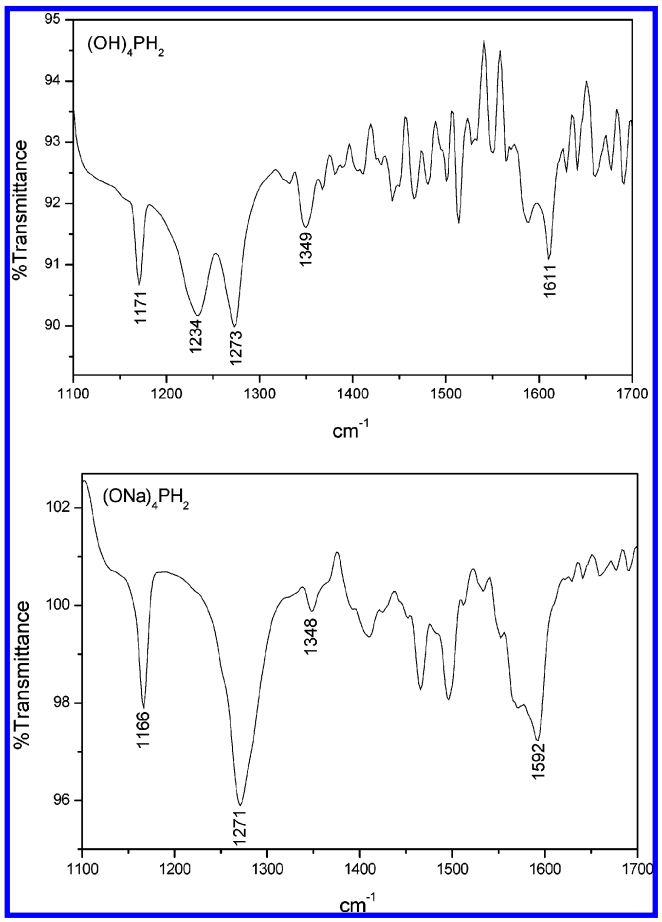

Figure 7. FT-IR spectra of $(OH)_4PH_2$ and $(ONa)_4PH_2$ in DMF + H_2O (1:1) mixture.

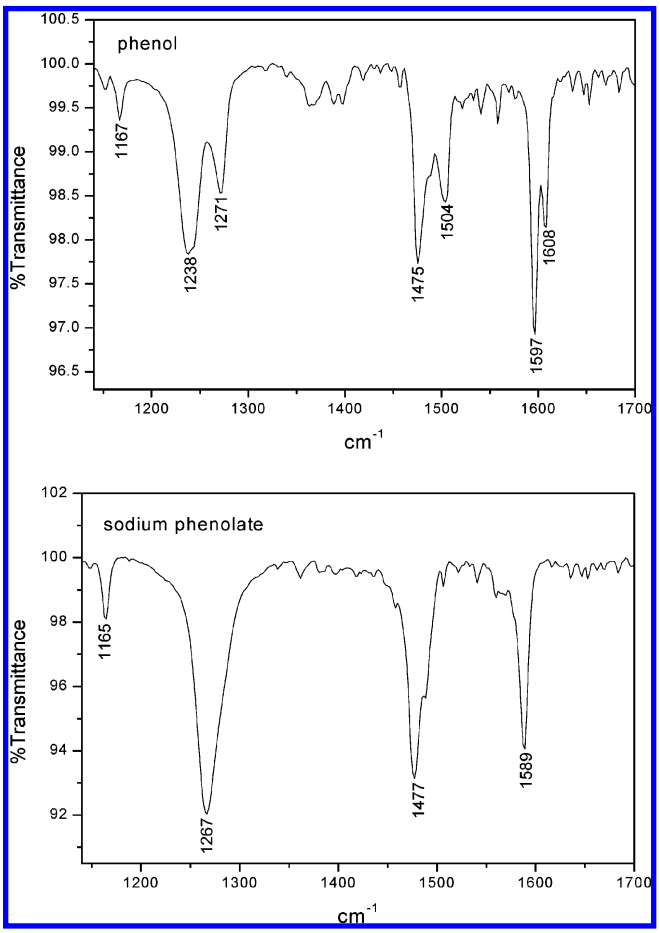

Figure 8. FT−IR spectra of phenol and sodium phenolate in a DMF + H_2O (1:1) mixture.

macrocycles remain essentially unperturbed. Therefore, the extra absorption bands can not possibly originate from Manna's "charge transfer state" but correspond to characteristics of hyperporphyrin spectra, which, based on different HOMOs or LUMOs due to charge localization, are generally considered to originate from charge-transfer transitions. In the p-type hyperporphyrins found with main-group metals in lower oxidation states, an extra orbital appears in the region of the HOMOs, and the extra bands are due to charge-transfer transitions $a_{2u}(np_z)$ (metal) $\rightarrow e_g(\pi^*)$ (ring); in the d-type hyperporphyrins found with transition metals in configurations d^m ($1 \leq m \leq 6$), extra orbitals appear among the LUMOs, and the extra bands are attributed to charge-transfer transitions $a_{1u}(\pi)$, $a_{2u}(\pi)$ (ring) $\rightarrow e_g(d_\pi)$ (metal).[3,7] Recent molecular orbital calculations on meso-tetrakis-(p-(dimethylamino)phenyl)porphyrin and its protonated forms suggest that the effect originates from π orbitals that are primarily localized on the aminophenyl substituent. These orbitals extend over the amino group as well as the phenyl π system and are calculated to correspond to HOMO and HOMO-1 for diprotonated meso-tetrakis-(p-(dimethylamino)-phenyl)porphyrin. The corresponding LUMO in these cases is a π^* orbital extending only over the porphyrin core. Thus, the lowest energy (hyperporphyrin) transition is assigned to π (aminophenyl) $\rightarrow \pi^*$(porphyrin), which can be interpreted as a charge-transfer transition. The reason that the π(aminophenyl) orbital appeared as the HOMO in these cases is a combination of the electron-donating effect of the amino group and the

SCHEME 2

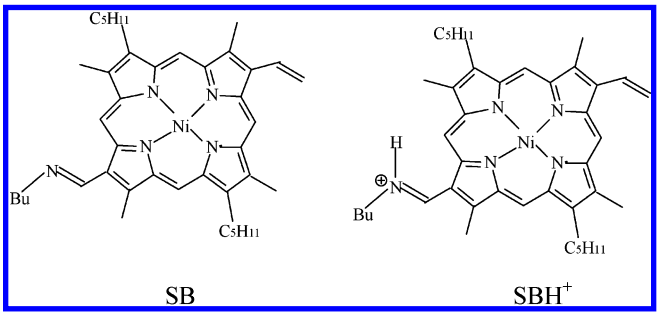

depression of core porphyrin π and π^* orbitals upon diprotonation.[8,9] In these sequentially deprotonated p-hydroxy substituted meso-tetraphenylporphyrins, we suggest that the negative charges on the phenoxide anion groups increase all the orbital energies, which has been demonstrated that meso-tetrakis-(3,5-di-*tert*-butyl-4-hydroxyphenyl)porphyrin undergoes facile aerial oxidation in basic solution to give novel diphenoquinoid tetrapyrrolic macrocycles. Hence, the $(ONa)_nPH_2$ complexes ought to be more difficult to reduce and easier to oxidize. However, deprotonation increases the energy of π orbitals localized on the phenoxide anion substituents proportionally more than that of the macrocycle π orbitals. Hence the phenoxide anion π orbital crosses over the porphyrin π orbital, creating a different HOMO and thereby a charge-transfer transition (π(phenoxide anion) $\rightarrow$ π^*(porphyrin)) at lower energy and in higher oscillator strength. This results in red-shifted, enhanced new bands in the visible region. Increasing deprotonation of the para-hydroxyphenyl increases the energy of π(phenoxide anion) orbital causing the charge-transfer transition (s) to lower energy. Therefore, the more phenoxide anions on the para-hydroxy substituted meso-tetraphenylporphyrins, the more the new bands in the optical spectra are red-shifted.

In the visible-near region, the splitting or broadening of the Soret band and its significant loss of oscillator strength upon deprotonation are observed, which are similar to the phenomena found in the case of metal complexes of Schiff base porphyrins (SB). Hanson et al.,[9,21] through the extensive calculations and analysis, related the spectral change to decrease in the energy of the SB π^* orbital caused by protonation. This leads to extensive mixing with one of the π^*(porphyrin) orbitals. Thus, the visible-near spectrum arises from transitions from two HOMO(π) orbitals to three LUMO(π^*) orbitals thereby qualitatively accounting for the observed split or broadened Soret bands. Here we give a similar interpretation that the spectral change in the visible-near region may originate from charge-transfer transitions π(phenoxide anion) $\rightarrow$ π^*(porphyrin) coming into the energy range of the normal π(porphyrin) $\rightarrow$ π^*(porphyrin) of the four-orbital model due to the HOMO (s) localized on the phenoxide anion substituent (s) close to π(porphyrin) in energy.

5. Summary

Meso-(p-hydroxyphenyl)porphyrins are a series of very important porphyrins because of their wide use for photosensitizers[22] in the model system of photosynthesis and for oxygen-reduction catalysis[4,11] (in fuel cells, as well as in solar energy conversion and storage systems). In particular, recently much interest has focused on their use in the photodynamic therapy of cancer.[23−25] It is fundamental, therefore, to understand the molecular origin bringing about red-shifted optical spectra in this porphyrin series under basic conditions. Despite several attempts to clarify the red-shifted phenomenon of the optical spectra of $(OH)_4PH_2$ in a basic solution,[8,19,20] the direct evidence that assign $(OH)_4PH_2$ as a hyperporphyrin has not been reported as yet. The present study provides RR and FTIR data that support $(OH)_4PH_2$ as a hyperporphyrin and extends this result to the whole meso-(p-hydroxyphenyl)porphyrin series.

The RR and FTIR data clearly indicate that for this porphyrin series the ground states of the macrocycles are not very much perturbed and that the charges are mainly localized on the substituents. This behavior of meso-(p-hydroxyphenyl)porphyrins is similar to that for protonated Schiff base porphyrins. Therefore, the unusual red shift of absorption maxima in the visible region and the Soret band splitting or broadening observed for all four porphyrins upon deprotonation is considered to be characteristic of hyperporphyrin spectra which are due to π(phenoxide anion) $\rightarrow$ π^*(porphyrin) transitions. To further fully understand the basified oxyphenylporphrins, detailed calculation is needed.

Acknowledgment. This work was supported by Special Funds for Major State Basic Research of China (No 2002CB-713803).

References and Notes

(1) Debus, R. J.; Barry, B. A.; Sithole, I.; Babcock, G. T.; McIntosh, L. *Biochemistry* **1988**, *27*, 9071−9074.

(2) Gentemann, S.; Medforth, C. J.; Forsyth, T. P.; Nurco, D. J.; Smith, K. M.; Fajer, J.; Holten, D. *J. Am. Chem. Soc.* **1994**, *116*, 7363−7368.

(3) Gouterman, M. In *The Porphyrins*; Dolphin, D., Ed.; Academic Press: New York, 1978; Vol. III, pp 1−165.

(4) Milgrom, L. R. *Tetrahedron* **1983**, *39*, 3895−3898.

(5) Datta-Gupta, N.; Bardos, T. J. *J. Heterocycl. Chem.* **1966**, *3*, 495−502.

(6) Gunter, M. J.; Robinson, B. C. *Aust. J. Chem.* **1989**, *42*, 1897−1905.

(7) Ojadi, E. C. A.; Linschitz, H.; Gouterman, M.; Walter, R. I.; Lindsey, J. S.; Wagner, R. W.; Droupadi, P. R.; Wang, W. *J. Phys. Chem.* **1993**, *97*, 13192−13197.

(8) Weinkauf, J. R.; Cooper, S. W.; Schweiger, A.; Wamser, C. C. *J. Phys. Chem. A* **2003**, *107*, 3486−3496.

(9) Vitasovic, M.; Gouterman, M.; Linschitz, H. *J. Porphyrins Phthalocyanines* **2001**, *5*, 191−197.

(10) Li, X.; Xu, Y.; Shi, Y.; Wang, X.; Guo, J.; Liu, G. *Ziran Kexue Jinzhan* **2002**, *12*, 201−204.

(11) Milgrom, L. R.; Jones, C. C.; Harriman, A. *J. Chem. Soc., Perkin Trans. 2* **1988**, 71−79.

(12) Zhang, Y.; Chen, D.; He, T.; Liu, F. *Spectrochim. Acta Part A* **2003**, *59*, 87−101.

(13) Li, X.; Czernuszewicz, R. S.; Kincaid, J. R.; Oliver Su, Y.; Spiro, T. G. *J. Phys. Chem.* **1990**, *94*, 31−47.

(14) Callahan, P. M.; Babcock, G. T. *Biochemistry* **1981**, *20*, 952−958.

(15) Hu, S.; Spiro, T. G. *J. Am. Chem. Soc.* **1993**, *115*, 12029−12034.

(16) Conley, R. T. *Infrared Spectroscopy*; Allyn and Bacon: Boston, 1966.

(17) Nonella, M.; Suter, H. U. *J. Phys. Chem. A* **1999**, *103*, 7867−7871.

(18) Ward, B.; Callahan, P. M.; Young, R.; Babcock, G. T.; Chang, C. K. *J. Am. Chem. Soc.* **1983**, *105*, 634−636.

(19) Manna, B. K.; Bera, S. C.; Rohatgi-Mukherjee, K. K. *Spectrochim. Acta* **1995**, *51A*, 1051−1060.

(20) Wasbotten, I. H.; Conradie, J.; Ghosh, A. *J. Phys. Chem. B* **2003**, *107*, 3613−3623.

(21) Hanson, L. K.; Chang, C. K.; Ward, B.; Callahan, P. M.; Babcock, G. T.; Head, J. D. *J. Am. Chem. Soc.* **1984**, *106*, 3950−3958.

(22) Neta, P.; Richoux, M. C.; Harriman, A.; Milgrom, L. R. *J. Chem. Soc., Faraday Trans.2* **1986**, *82*, 209−217.

(23) Ferrand, Y.; Bourre, L.; Simonneaux, G.; Thibaut, S.; Odobel, F.; Lajat, Y.; Patrice, T. *Bioorganic & Medicinal Chemistry Lett.* **2003**, *13*, 833−835.

(24) Zhang, J.; Wu, X.; Gao, X.; Yang, F.; Wang, J.; Zhou, X.; Zhang, X. *Bioorg. Med. Chem. Lett.* **2003**, *13*, 1097−1100.

(25) Sharman, W. M.; Van Lier, J. E.; Allen, C. M. *Adv. Drug Delivery Rev.* **2004**, *56*, 53−76.